

# Theoretical and experimental demonstration of the existence of quadrupole Cooper Minima

P C Deshmukh<sup>1</sup>, T Banerjee<sup>1</sup>, H R Varma<sup>1</sup>, O Hemmers<sup>2</sup>, R Guillemin<sup>2</sup>‡, D Rolles<sup>3</sup>§, A Wolska<sup>2</sup>||, S W Yu<sup>2,3</sup>¶, D W Lindle<sup>2</sup>, W R Johnson<sup>4</sup> and S T Manson<sup>5</sup>

<sup>1</sup> Department of Physics, Indian Institute of Technology-Madras, Chennai 600036

<sup>2</sup> Department of Chemistry, University of Nevada, Las Vegas, NV 89154-4003

<sup>3</sup> Advanced Light Source, Lawrence Berkeley National Laboratory, Berkeley, California 94720

<sup>4</sup> Department of Physics, University of Notre Dame, Notre Dame, Indiana 46556

<sup>5</sup> Department of Physics and Astronomy, Georgia State University, Atlanta, GA 30303-3083

E-mail: [hemmers@unlv.nevada.edu](mailto:hemmers@unlv.nevada.edu)

**Abstract.** Calculations and measurements of the Xe 5s and 5p nondipole photoelectron asymmetry parameters are obtained which present clear evidence of the existence of *quadrupole* Cooper minima, i.e., minima in quadrupole matrix elements as a function of energy, in the photoionization process. This verifies earlier predictions of quadrupole Cooper Minima.

‡ Present address: Laboratoire de Chimie Physique-Matière et Rayonnement, UMR 7614, 75231 Paris Cedex 05, France

§ Present address: Physics Department, Western Michigan University, Kalamazoo, Michigan 49008, USA

|| Present address: Institute of Physics, Polish Academy of Sciences, Al. Lotnikow 32/46, 02-668 Warsaw, Poland

¶ Present address: University of California, Lawrence Livermore National Laboratory, Livermore, California 94550, USA

Laboratory studies of nondipole effects in photoionization have seen a recent renaissance owing to the unparalleled brightness of modern light sources that have made such precision investigations possible [1]. Studies of low-energy nondipole effects in atomic photoionization reveal information about quadrupole-allowed ionization channels and the elusive quadrupole ionization process itself because the nondipole angular-distribution parameters depend upon interferences between quadrupole and dipole matrix elements [2, 3, 4, 5].

Atoms, owing to their relative simplicity, are the ideal target for these studies because they generally allow for unambiguous interpretation of the results. In addition, atoms are simple enough to perform calculations approaching exactness. These investigations have significantly altered our understanding of nondipole effects in photoionization [1, 6, 7, 8, 9, 10, 11, 12, 13, 14, 15, 16, 17, 18, 19], which were previously thought to be of importance only at photon energies of many keV [20, 21, 22]. Furthermore, the effects of correlation in the quadrupole photoionization channels in the form of interchannel coupling and quadrupole ionization plus excitation (satellite) channels were inferred as a result of combined experimental and theoretical studies [17]. In addition, for dipole photoionization, studies in regions of the well-known Cooper minima [23], i.e., zeros or near-zeros in dipole matrix elements, have proved extremely useful as benchmarks because the various photoionization parameters take on well-defined values at these minima. Moreover, the quantitative details of matrix element minima are extremely sensitive to many-body correlations. Similar considerations must also apply for *quadrupole* Cooper minima.

In this letter, we report experimental evidence for the existence of a quadrupole Cooper minimum, the result of a combined laboratory and computational investigation of nondipole effects in Xe valence-shell photoionization. Note that quadrupole Cooper minima have been predicted for some time [24], but without experimental confirmation. This investigation is an example of how a combined experimental/theoretical study can yield significantly more insight than the sum of individual experimental and theoretical investigations.

The differential cross section for photoionization, including the lowest-order nondipole contribution, is given by [3, 4, 25, 26, 27]

$$\frac{d\sigma}{d\Omega}(\theta, \phi) = \frac{\sigma}{4\pi} \left\{ 1 + \beta P_2(\cos \theta) + (\delta + \gamma \cos^2 \theta) \sin \theta \cos \phi \right\}, \quad (1)$$

where  $\sigma$  is the angle-integrated cross section,  $\beta$  is the dipole anisotropy parameter,  $P_2(\cos \theta) = (3 \cos^2 \theta - 1)/2$ , and  $\delta$  and  $\gamma$  are first-order nondipole asymmetry parameters. The coordinate axes have the positive x-axis along the direction of the photon propagation vector, the z-axis along the photon polarization vector, and  $\theta$  and  $\phi$  are the polar and azimuthal angles of the photoelectron momentum vector. The dipole angular distribution parameter  $\beta$  depends only on ratios of dipole matrix elements, along with cosines of phase-shift differences. The nondipole parameters  $\gamma$  and  $\delta$  are given by sums of ratios of quadrupole ( $Q_{\nu}$ ) to dipole ( $D_{\nu'}$ ) transition matrix elements multiplied by the cosines of their phase-shift differences [3, 4, 5, 25, 26]. Thus, when the

dominant quadrupole matrix elements are small or zero, i.e, in the neighborhood of a Cooper minimum in the dominant quadrupole channel, it is evident that the nondipole parameters are near zero as well.

Specifically, for a transition in a closed-shell (or one-electron) atom  $n_b\kappa_b \rightarrow \epsilon\kappa$ ,  $\gamma$  is given (in atomic units) by [5]

$$\gamma = -\frac{k}{\bar{\sigma}} \sqrt{105} \sum_{\kappa, \kappa'} \langle \kappa' \| C_3 \| \kappa \rangle (-1)^{j'+j_b} \left\{ \begin{matrix} 1 & 2 & 3 \\ j' & j & j_b \end{matrix} \right\} \Im(D_\kappa Q_{\kappa'}^*), \quad (2)$$

where  $k$  ( $= \omega c$ ,  $\omega$  being the photon energy and  $c$  the speed of light) is the photon wave number,  $\bar{\sigma} = \sum |D_\kappa|^2$  (where we have assumed that the electric dipole cross section overshadows the magnetic dipole(e1) and electric quadrupole(e2) contributions), and  $\Im$  is the imaginary part of  $(D_\kappa Q_{\kappa'}^*)$ . The electric dipole and quadrupole amplitudes,  $D_\kappa$  and  $Q_{\kappa'}$  respectively, are given by

$$D_\kappa = i^{-\ell+1} \langle \epsilon\kappa \| r C_1 \| n_b\kappa_b \rangle e^{\delta_\kappa}, \quad (3)$$

$$Q_{\kappa'} = i^{-\ell'+1} \langle \epsilon\kappa' \| r^2 C_1 \| n_b\kappa_b \rangle e^{\delta_{\kappa'}} \quad (4)$$

with  $\delta_\kappa$  ( $\delta_{\kappa'}$ ) the continuum phase shift and  $\ell$  ( $\ell'$ ) the continuum orbital angular momentum. For initial  $ns$ -states,  $j_b=1/2$  and the expression for  $\gamma$  reduces to

$$\gamma = \frac{3k}{5} \frac{6R_{\frac{3}{2}}^{(1)} R_{\frac{3}{2}}^{(2)} \cos\Delta_{\frac{3}{2}, \frac{3}{2}} + 5R_{\frac{1}{2}}^{(1)} R_{\frac{5}{2}}^{(2)} \cos\Delta_{\frac{1}{2}, \frac{5}{2}} + 4R_{\frac{3}{2}}^{(1)} R_{\frac{5}{2}}^{(2)} \cos\Delta_{\frac{3}{2}, \frac{5}{2}}}{R_{\frac{1}{2}}^{(1)2} + 2R_{\frac{3}{2}}^{(2)2}} \quad (5)$$

with  $R_j^{(1)}$  and  $R_j^{(2)}$  the absolute values of the radial part of the dipole and quadrupole matrix elements, respectively, and  $\Delta_{j,j'} = \delta_j^{(1)} - \delta_{j'}^{(2)}$ , the phase shift differences between dipole and quadrupole channels. Finally, in the nonrelativistic limit, where the matrix elements and phase-shifts are independent of  $j$ ,  $\gamma$  reduces to the well-known nonrelativistic expression [4]

$$\gamma = 3k \frac{R^{(2)}}{R^{(1)}} \cos\Delta. \quad (6)$$

Calculations have been performed for the  $5p$  and  $5s$  states of Xe using the relativistic random phase approximation (RRPA) methodology which included coupling among *all* of the single excitation channels from  $5p$ ,  $5s$ ,  $4d$ ,  $4p$  and  $4s$  subshells, a total of 21 coupled relativistic dipole channels, and 25 coupled quadrupole channels. These calculations are similar to those of reference [14], except here *experimental* thresholds are used to allow for unambiguous comparison with experiment; otherwise, the calculations are entirely *ab initio*.

Measurements on Xe over the 80–215 eV photon energy range were made at Lawrence Berkeley National Laboratory's Advanced Light Source (ALS). In the experiment, electron analyzers were positioned at sets of angles that are sensitive to different combinations of  $\beta$ ,  $\delta$ , and  $\gamma$ , and ratios of the photoelectron intensities yielded values of  $\gamma + 3\delta$ . The measurement, performed on undulator beam line 8.0.1.3, used a gas-phase time-of-flight (TOF) photoelectron-spectroscopy system designed specifically

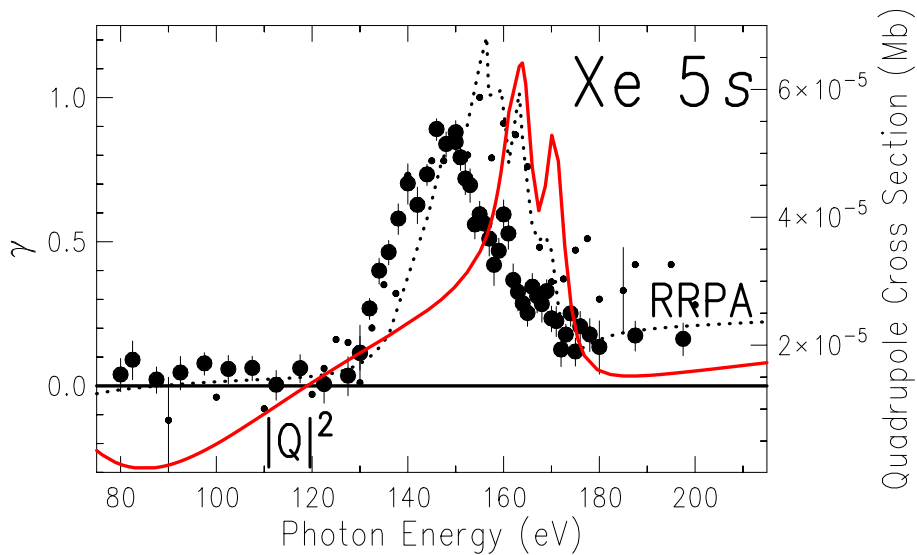


**Figure 1.** Xe 5s nondipole asymmetry parameter  $\gamma$  (left scale) measured at the ALS (large solid points) compared with our RRPA calculation (dotted curve) and experimental data (small solid points) from reference [13]. Also shown is our calculated RRPA *quadrupole* cross section (solid curve, right scale).

for soft-x-ray work at the ALS. A complete discussion of this apparatus is published elsewhere [28]. A key characteristic for the present measurements is the TOF method can measure photoelectron peaks at many kinetic energies and at multiple emission angles simultaneously, permitting sensitive determinations of cross-section ratios and electron angular distributions with minimal experimental uncertainty. It was important to separate the Xe 5s, 5p, and satellite lines for accurate measurements of the 5p angular distributions. Therefore, retarding voltages were applied to slow the electrons and gain resolution. Helium 1s and neon 2s photolines were used to calibrate the analyzers because the dipole and nondipole angular distributions are well known for helium 1s and neon 2s [4]. They were also used to determine the degree of linear polarization of the synchrotron light, which has been determined to be better than 99.9 %.

The  $\gamma$  parameter for Xe 5s [15] measured at the ALS is shown in Fig. 1 along with our RRPA results;  $\delta$  vanishes for *s*-states. Here relatively good agreement between theory and experiment is seen, both in the region of the structure in the 130 eV to 180 eV range, and below 130 eV where the  $\gamma$  parameter is essentially zero. The  $\gamma$  parameter for *ns* photoionization is proportional to the ratio of the quadrupole to dipole matrix element, in a nonrelativistic formulation [4], as delineated above. Thus, the zero value of  $\gamma$  indicates the possibility of a minimum in the quadrupole matrix element. The calculated quadrupole cross section is also shown in Fig. 1, and a quadrupole Cooper minimum is predicted at a photon energy of about 87 eV, uncomplicated by any resonance or interchannel structures, thereby serving to strongly suggest the zero value of the  $\gamma$  parameter is indeed the result of a quadrupole Cooper minimum.

Note however, even though the Cooper minimum in the quadrupole manifold

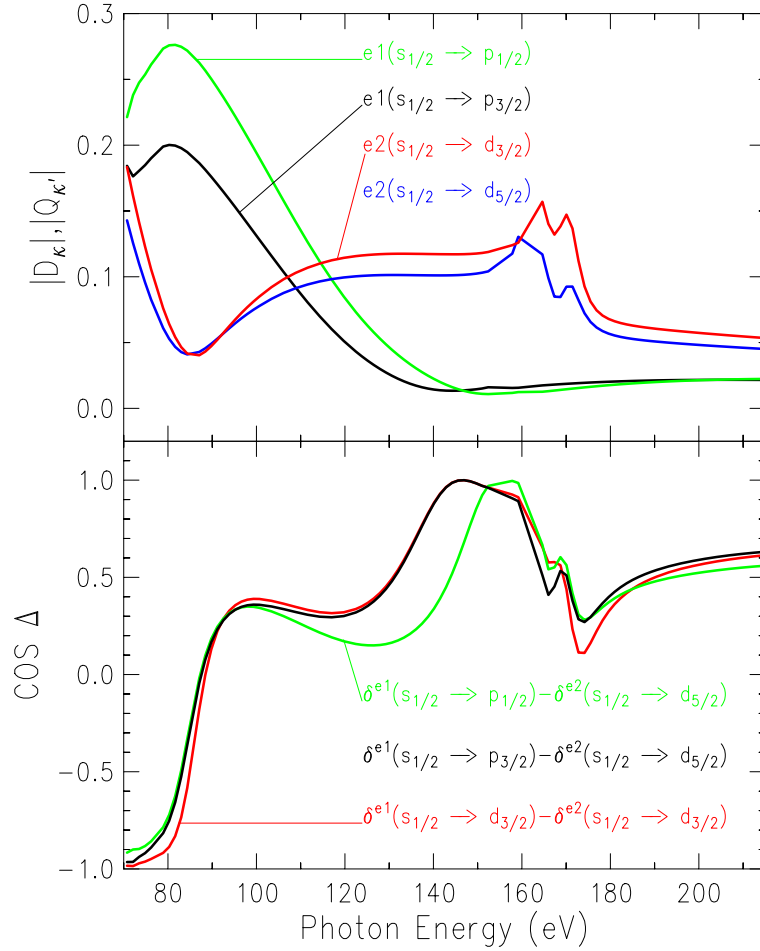


**Figure 2.** Absolute values of the calculated Xe 5s dipole and quadrupole matrix elements (upper panel) and cosines of the phase-shift differences (lower panel).

appears at 87 eV, the  $\gamma$  parameter is near zero over a broad range from 75 eV to 125 eV, as seen in Fig. 1. This occurs because the quadrupole matrix elements are continuous functions of energy; the existence of the Cooper minimum depresses the value of the quadrupole matrix elements and, thereby, the quadrupole cross section, over a broad range in the neighborhood of the Cooper minimum. This behavior is well-known for dipole Cooper minima [29]. The quadrupole cross section remains anomalously small, compared to the dipole cross section, over a broad energy region. In fact, the calculation shows the  $\gamma$  parameter has a value of about -0.025 at 75 eV photon energy, then goes through a zero around 87 eV, and rises to a positive value of 0.04 near 125 eV. Thus, although the nondipole  $\gamma$  parameter is only zero at a single energy in this region, the values of  $\gamma$  over the entire 75 – 125 eV region are so small they cannot be observed with the sensitivity of the present experiment.

To understand this behavior in detail, it is necessary to scrutinize the individual relativistic dipole and quadrupole matrix elements, along with the cosines of the phase-shift differences as well. The relevant matrix elements and cosines are shown in Fig. 2,

where it is seen both relativistic quadrupole matrix elements exhibit Cooper minima in the 85 eV region; these result in the Cooper minimum in the quadrupole cross section displayed in Fig. 1. Below the Cooper minima, at 80 eV, the cosines, shown in Fig. 2, are seen to be negative but of order unity, so the vanishing value of  $\gamma$  is due to the approach to the Cooper minima in the quadrupole matrix elements. Absent the quadrupole Cooper minima, if the quadrupole and dipole matrix elements were the same size with the cosines  $\sim -1$ , then the value of  $\gamma$  would be about 0.1, a value that could be seen experimentally. In the narrow vicinity of the Cooper minima, the cosines are seen to rapidly change sign; this is simply because the quadrupole matrix elements become complex when interchannel coupling is included, so when the real parts of the matrix elements go through zero, the cosines change sign. In contrast, the dipole phases are relatively constant in this region.

Above the Cooper minima, Fig. 2 shows the cosines take on values of  $\sim 0.5$ . Thus, when the quadrupole matrix elements "recover" from the Cooper minima and are about the same magnitude as the dipole, which occurs near 120 eV, the cosines suppress the value of  $\gamma$  so it is too small to be seen experimentally. Only when the quadrupole matrix elements become at least a factor of two larger than the dipole, at around 130 eV, is a deviation from the zero value of  $\gamma$  exhibited experimentally. In other words, the measured zero value of  $\gamma$  over the energy region from about 75 - 120 eV results from the quadrupole Cooper minima, but the 120 - 130 eV region is due to a combination of the quadrupole Cooper minima and the cosines of the phase-shift differences.

Above 125 eV, the dipole channel develops a Cooper minimum, which dramatically reduces the dipole matrix element and cross section. This, in turn, causes the ratio of the quadrupole to dipole matrix element to correspondingly increase, thereby producing the structure in  $\gamma$  above 125 eV shown in Fig. 1.

The results of the present measurement of the Xe  $5p$   $\zeta$  ( $= \gamma + 3\delta$ ), and the comparison with the RRPA calculation are shown in Fig. 3. Over the broad energy range shown, agreement between theory and experiment is quite poor. Because it is known that the integrated cross section, the dipole angular-distribution parameter  $\beta$ , and the  $5p_{3/2}:5p_{1/2}$  branching ratio are predicted quite well by the RRPA calculation [29], the difficulty must be in the quadrupole channels. The quadrupole calculation, however, includes *all* relevant single-ionization channels, along with the interchannel coupling among them. Thus, the problem seems to be omission of multiple-excitation channels within the quadrupole manifold, i.e., the absence of quadrupole satellite channels. But, satellite channels typically are important only when the single-particle channels are, for some reason, small. And, in this case, the  $5p$  quadrupole single-ionization cross section should not be small owing to the  $5p \rightarrow \epsilon f$  quadrupole transitions which should be large because the  $f$ -wave is resonant in Xe, i.e., the  $f$ -wave is known from Xe  $4d$  photoionization to exhibit a strong shape resonance extending over a broad energy range [29]. It is, therefore, difficult to understand how the (omitted) satellite channels could be of importance; a situation that would require the  $5p \rightarrow \epsilon f$  quadrupole transitions to be anomalously small.

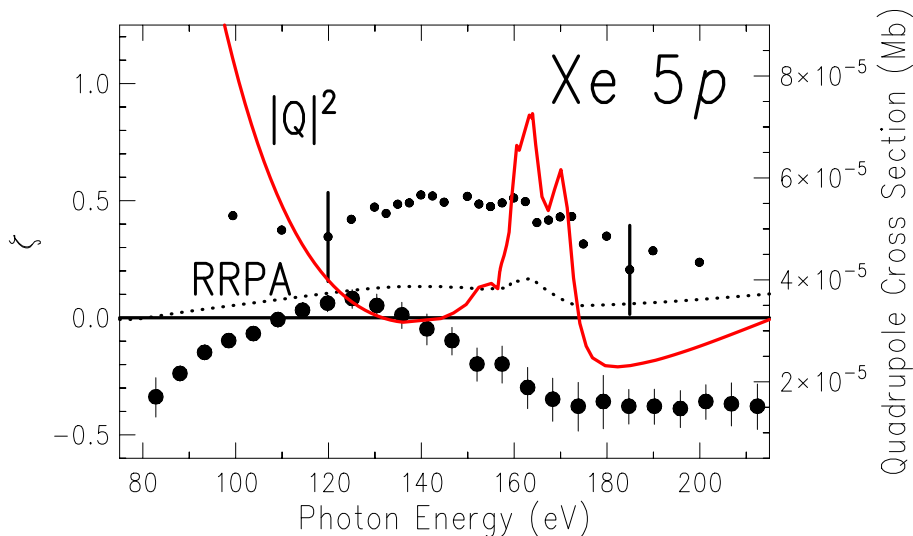


**Figure 3.** Xe  $5p$  nondipole asymmetry parameter  $\zeta$  (left scale) measured at ALS (large solid points) compared with our RRPA calculation (dotted curve) and experimental data (small solid points) from reference [31]. Also shown is our calculated RRPA *quadrupole* cross section (solid curve, right scale)

Our calculations shed light on this conundrum. Although these transitions are resonant, the RRPA results predict a *quadrupole* Cooper minimum in the 120 – 160 eV photon-energy region, thereby causing the  $5p$  quadrupole cross section to be anomalously small over a broad range of energy, as seen in Fig. 3 where the  $5p$  RRPA quadrupole cross section is also shown. The *quadrupole* cross section is seen to reach a minimum of about 20 barns; the structure in this region is due to interchannel coupling with  $4p$  quadrupole transitions. In any case, the disagreement between theory and experiment is evidently due to the omission of the relatively strong satellite transitions leading to the  $4d^84f$  excited states of  $\text{Xe}^+$  [17, 30], engendered by the smallness of the  $5p$  quadrupole cross section owing to the Cooper minimum. As for Xe  $5s$ , the nondipole parameter  $\zeta$  for  $5p$  is close to zero in the range of the Cooper minimum. This result, thus, provides further experimental evidence, albeit indirect, for the existence of a quadrupole Cooper minimum.

Another measurement for Xe  $5p$  has been reported [31] which disagrees with our present results (and with theory). Over the past decade we have created a significant body of measurements of nondipole effects on less complex systems [8, 10, 32] where our results agree well with theory; in fact several different theoretical calculations agree with each other and our earlier measurements [8, 10, 32]. Furthermore, our data show excellent agreement with the results of another experimental group [15] that also has many years of experience in the field [6, 7, 12]. For these reasons we have confidence in our present experimental results, and not just because our error bars are smaller than those of reference [31]. We do not have any explanation for the difference between our present results and those of reference [31].

In summary, clear indications of quadrupole Cooper minima are demonstrated *via* a combination of theory and experiment, thereby confirming a prediction made some time ago [24]. In addition, our results indicate insight can be gained from the juxtaposition of theory and experiment that cannot be garnered from either alone. Studies of quadrupole Cooper minima offer an excellent opportunity to understand correlation in the quadrupole manifold. In the present investigation, for example, the importance of quadrupole satellite transitions in a new case has been demonstrated. Finally, atoms are merely the laboratory to study quadrupole phenomenology. These results should be applicable to molecules, clusters, surfaces, and bulk condensed matter as well.

## Acknowledgments

Helpful discussions with R. H. Pratt and L. A. LaJohn are gratefully acknowledged. The ITT group was supported in part by a joint DST (India) and NSF (US) grant. The UNLV group acknowledges support by NSF Grant No. PHY-0555699. DR acknowledges the financial support through the ALS Doctoral Fellowship in Residence program. The research of WRJ was supported in part by NSF Grant No. PHY04-56828. The work of STM was supported by DOE, Division of Chemical Sciences, BES grant No. DE-FG02-03ER15428. The ALS (LBNL) was supported by DOE, Materials Science Division, BES, OER under Contract No. DE-AC03-76SF00098.

## References

- [1] Guillemin R, Hemmers O, Lindle D W and Manson S T 2005 *Radiation Phys. Chem.* **73** 311 and references therein
- [2] Amusia M Ya and Cherepkov N A 1975 *Case Stud. Atomic Phys.* **5** 47 and references therein
- [3] Bechler A and Pratt R H 1989 *Phys. Rev. A* **39** 1774; Bechler A and Pratt R H 1990 **42** 6400 and references therein
- [4] Cooper J W 1990 *Phys. Rev. A* **42** 6942; Cooper J W 1992 *Phys. Rev. A* **45** 3362; Cooper J W 1993 *Phys. Rev. A* **47** 1841 and references therein
- [5] Derevianko A, Johnson W R and Cheng K T, 1999 *At. Data Nuc. Data Tables* **23** 153 and references therein
- [6] Krässig B, Jung M, Gemmell D S, Kanter E P, LeBrun T, Southworth S H and Young L 1995 *Phys. Rev. Lett.* **75** 4736
- [7] Jung M, Krässig B, Gemmell D S, Kanter E P, LeBrun T, Southworth S H and Young L 1996 *Phys. Rev. A* **54** 2127
- [8] Hemmers O, Fisher G, Glans P, Hansen D L, Wang H, Whitfield S B, Wehlitz R, Levin J C, Sellin I A, Perera R C C, Dias E W B, Chakraborty H S, Deshmukh P C, Manson S T and Lindle D W 1997 *J. Phys. B* **30** L727
- [9] Dolmatov V K and Manson S T 1999 *Phys. Rev. Lett.* **83** 939
- [10] Derevianko A, Hemmers O, Oblad S, Glans P, Wang H, Whitfield S B, Wehlitz R, Sellin I A, Johnson W R and Lindle D W 2000 *Phys. Rev. Lett.* **84** 2116
- [11] Amusia M Ya, Baltakov A S, Chernysheva L V, Felfli Z and Msezane A Z 2001 *Phys. Rev. A* **63** 052506

- [12] Krässig B, Kanter E P, Southworth S H, Guillemin R, Hemmers O, Lindle D W, Wehlitz R and Martin N L S 2002 *Phys. Rev. Lett.* **88** 203002
- [13] Risz S, Sankari R, Kövèr À, Jurvansuu M, Varga D, Nikkinen J, Ricsoka T, Aksela H and Aksela S 2003 *Phys. Rev. A* **67** 012712
- [14] Johnson W R and Cheng K T 2001 *Phys. Rev. A* **63** 022504
- [15] Hemmers O, Guillemin R, Kanter E P, Krässig B, Lindle D W, Southworth S H, Wehlitz R, Baker J, Hudson A, Lotrakul M, Rolles D, Stolte W C, Tran I C, Wolska A, Yu S W, Amusia M Ya, Cheng K T, Chernysheva L V, Johnson W R and Manson S T 2003 *Phys. Rev. Lett.* **91** 053002
- [16] Dolmatov V K, Baltenkov A S and Manson S T 2003 *Phys. Rev. A* **67** 062714
- [17] Hemmers O, Guillemin R, Rolles D, Wolska A, Lindle D W, Cheng K T, Johnson W R, Zhou H L and Manson S T 2004 *Phys. Rev. Lett.* **93** 113001
- [18] Saha H P 2004 *Phys. Rev. A* **69** 022712
- [19] Dolmatov V K, Bailey D and Manson S T 2005 *Phys. Rev. A* **72** 022718
- [20] Bethe H A and Salpeter E E 1958 *Quantum Mechanics of One- and Two-Electron Atoms* (Berlin: Springer-Verlag) p 248ff
- [21] Manson S T and Dill D 1978 *Electron Spectroscopy: Theory, Techniques and Applications* vol 2 ed C R Brundle and A D Baker (New York: Academic Press) p 157-195
- [22] Starace A F 1982 *Handbuch der Physik* vol 31 ed W Mehlhorn (Berlin: Springer-Verlag) p 1-121
- [23] Cooper J W 1962 *Phys. Rev.* **128** 681
- [24] Wang M S, Kim Y S, Pratt R H, and Ron A, 1982 *Phys. Rev. A* **25** 857
- [25] Amusia M Ya, Arifov P U, Baltenkov A S, Grinberg A A and Shapiro S G 1974 *Phys. Lett.* **47A** 66
- [26] Amusia M Ya and Dolmatov V K 1980 *Sov. Phys. JETP* **52** 840
- [27] Peshkin M 1970 *Adv. Chem. Phys.* **18** 1
- [28] Hemmers O, Whitfield S B, Glans P, Wang H, Lindle D W, Wehlitz R and Sellin I A 1998 *Rev. Sci. Instrum.* **69** 3809
- [29] Schmidt V 1992 *Rep. Prog. Phys.* **55** 1484 and references therein
- [30] Smid H and Hansen J 1987 *J. Phys. B* **20** 6541
- [31] Sankari R, Risz S, Kövèr À, Jurvansuu M, Varga D, Nikkinen J, Ricsoka T, Aksela H and Aksela S 2004 *Phys. Rev. A* **69** 012707
- [32] Johnson W R, Derevianko A, Cheng K T, Dolmatov V K and Manson S T 1999 *Phys. Rev. A* **59** 3609